Effects of Fiber Orientation on Mechanical and Electrical Properties of a Polystyrene-Carbon Nanofiber Composite Material

Honors Thesis for Graduation With Distinction

Submitted May 2007

By Steve Gronauer

The Ohio State University

Department of Chemical and Biomolecular Engineering

140 West 19th Avenue

Columbus, OH 43210

Honors Committee:

Dr. Kurt Koelling, Advisor

Dr. Stephen Bechtel

Acknowledgements

I would like to thank everyone who helped make it possible for me to work on this project for the past year. First, I would like to thank Dr. Kurt Koelling and Dr. Stephen Bechtel for giving me the opportunity to learn about their research and undertake this project. Second, I owe a huge thank you to Chris Kagarise. Chris was the person with whom I worked most closely on this project, and without his help I would have been totally lost. I would also like to thank Monon Mahboob specifically for his help with AutoCAD, a program with which I had very little experience. Finally, although I did not work alongside of him, I would like to thank Jianhua Xu for writing the AutoCAD program that saved me from having to count individual fiber lengths and angles in every picture.

Outside of the research group, the people to whom I owe the most gratitude are my family and friends. My family, especially my parents, gave me the opportunity to attend Ohio State and pursue my degree. My friends in the Chemical Engineering major helped me through four challenging years, and I had friends both inside and outside of the major helping me to relax outside of school. Finally, I would like to thank my girlfriend, Jen Kaufhold, for being there when classes were stressful, and for at least pretending to be interested when I talk about things like fiber orientation and polymer materials. You have all been tremendously helpful in one way or another, and you have enabled me to gain valuable experience in chemical engineering research.

Abstract

Polystyrene can be reinforced with nanoparticles to enhance the physical properties of the material. Carbon nanofibers are a lower-cost nanoparticle that improve the mechanical and electrical properties of polymer materials. Materials of varying compositions (0, 2, 5, or 10 wt% carbon nanofibers) were studied to examine the effects of composition on tensile strength and electrical resistivity. In addition, processing method was varied (compression molding or injection molding); furthermore, injection molded samples were injected at different speeds (0.75, 1.5, 2.25, or 3 in/s). These processing parameters were adjusted to create different carbon nanofiber orientations to study the effects of fiber orientation on tensile strength and electrical resistivity. Finally, samples were deformed to study the effects of shear strain on fiber orientation.

It was concluded that composition and injection speed both significantly affected tensile strength, while tensile modulus was significantly affected by composition only. Composition also significantly affected electrical resistivity. Processing method alone did not have a significant effect on resistivity, though it did significantly interact with composition. Injection speed did not appear to have a significant effect on resistivity, though this conclusion could be due to a small range of injection speeds. Orientation tensors, along with their corresponding eigenvalues and eigenvectors, were calculated for samples subjected to extensional shear. The carbon nanofibers tended to align more in the direction of flow as total strain increased; however, at a certain point, adding more strain ceased to have a significant effect on fiber orientation.

Table of Contents

List of Figures

1) Introduction

Nanoparticle-reinforced composites have been an important innovation in the field of polymer science over the past few decades. Adding nanoparticles to a polymer system can greatly enhance the physical properties of the material. In many cases, the nanoparticle that is used in the system is some type of carbon fiber. Two major types of carbon fiber are relevant to this application: the single-wall carbon nanotube and the carbon nanofiber. Both of these materials consist of graphene, which is a planar arrangement of carbon atoms bonded to one another in an sp^2 geometry. In the single-wall carbon nanotube, the graphene wraps around into a cylindrical arrangement. The carbon nanofiber, however, is basically a stack of these graphene sheets that have been arranged in a cone formation. Figure 1.1 shows a side-by-side comparison of the geometries of the two types of fibers.

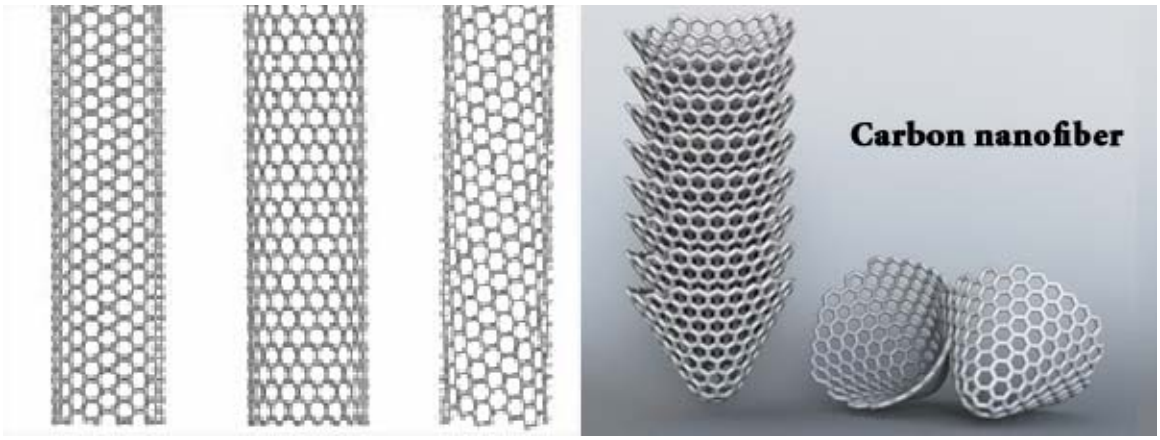

Figure 1.1: Geometry of Single-Wall Carbon Nanotubes (from http://polymers.nsel.nist.gov) and Carbon Nanofibers (from http://www.den.hokudai.ac.jp)

The single-wall carbon nanotube, shown at left in Figure 1.1, was one of the first nanoparticles to be utilized in this manner. Adding even a small weight percentage of single-walled carbon nanotubes can enhance the mechanical strength of a polymer material, as well as the thermal and electrical conductivity. However, it was later found

that carbon nanofibers provide a less expensive alternative with similar enhancement of properties.

A nanofiber-reinforced polymer material that has been studied at length is a system of carbon nanofibers in polystyrene. This material has applications as a semiconductive thermoplastic that can be used in computer housings or automobile bumpers, among other applications. Previous research has focused on the physical properties of the solid material, and some more recent work has explored the rheological properties of this material in its liquid phase, which is the phase in which it is processed.

One important property of the carbon nanofiber/polystyrene system is the geometric orientation of the nanofibers in the polystyrene. When there is more contact between neighboring nanofibers, previous research suggests that the electrical and thermal conductivities increase, as does the material strength. The main factor that determines how the nanofibers are oriented is the processing method used. Two main processing methods are widely used: compression molding and injection molding. Compression molding, in theory, should produce a mostly random arrangement of nanofibers, since the mold is filled in a very random manner. However, if injection molding is used, it is possible that the material will experience enough shear that the nanofibers will, at least partially, be oriented in the direction of flow. Additional factors, such as deformation or stretching, could also contribute to the orientation of the nanofibers after the material is processed.

One important way to quantify the orientation of the carbon nanofibers is the orientation tensor. The orientation tensor numerically shows the tendency of the nanofibers in a system to be aligned in a certain direction. In order to determine the

orientation tensor, an image of the system is needed. The images for this study were taken using transmission electron microscopy (TEM). The in-plane angle, ϕ, of each nanofiber can be easily determined with a simple measurement. However, in order to find the out-of-plane angle, θ, a calculation is required. On the image, each fiber has a projected length, L. The out-of-plane angle can be found with the following equation:

$$\theta = \tan^{-1}(L/t)\,, \textbf{(1.1)}$$

where t is the thickness of the slice being analyzed. This equation uses the assumption that when the material is sliced, each fiber is cut on both ends, and so every fiber has a length equal to the slice thickness. Once the two angles have been determined, they must both be corrected before they can be used to calculate the orientation tensor. The corrections are as follows:

$$\phi_c = \frac{180}{\pi}\tan^{-1}\left(\cos\left(\frac{\alpha\pi}{180}\right)\sin\left(\frac{\theta\pi}{180}\right)\sin\left(\frac{\phi\pi}{180}\right) - \frac{\sin\left(\frac{\alpha\pi}{180}\right)\cos\left(\frac{\phi\pi}{180}\right)}{\sin\left(\frac{\theta\pi}{180}\right)\cos\left(\frac{\phi\pi}{180}\right)}\right), \textbf{(1.2)}$$

$$\theta_c = \frac{180}{\pi}\cos^{-1}\left(\sin\left(\frac{\alpha\pi}{180}\right)\sin\left(\frac{\theta\pi}{180}\right)\sin\left(\frac{\phi\pi}{180}\right) + \cos\left(\frac{\alpha\pi}{180}\right)\cos\left(\frac{\theta\pi}{180}\right)\right), \textbf{(1.3)}$$

In both of the above equations, α represents the complement of the angle between the cut and the flow direction. This correction accounts for the fact that the angles calculated by the AutoCAD code are not the same as the actual angles of the fibers within the sample. Once these corrected angles are obtained, the orientation tensor can be calculated. It is important to note that the orientation tensor is symmetric, so corresponding off-diagonal entries will be equal to one another. The direction of flow (in the case of this study, the length of the sample) is taken to be the 1-direction, while the width of the sample is the 2-

direction and the thickness of the sample is the 3-direction. The following equations are used to calculate the orientation tensor:

$$a_{11} = \left(\cos\left(\frac{\phi_c \pi}{180}\right) \sin\left(\frac{\theta_c \pi}{180}\right) \right)^2, \textbf{(1.4)}$$

$$a_{22} = \left(\sin\left(\frac{\phi_c \pi}{180}\right) \sin\left(\frac{\theta_c \pi}{180}\right) \right)^2, \textbf{(1.5)}$$

$$a_{33} = \cos^2\left(\frac{\theta_c \pi}{180}\right), \textbf{(1.6)}$$

$$a_{12} = a_{21} = \sin^2\left(\frac{\theta_c \pi}{180}\right) \sin\left(\frac{\phi_c \pi}{180}\right) \cos\left(\frac{\phi_c \pi}{180}\right), \textbf{(1.7)}$$

$$a_{13} = a_{31} = \sin\left(\frac{\theta_c \pi}{180}\right) \cos\left(\frac{\theta_c \pi}{180}\right) \cos\left(\frac{\phi_c \pi}{180}\right), \textbf{(1.8)}$$

$$a_{23} = a_{32} = \sin\left(\frac{\theta_c \pi}{180}\right) \cos\left(\frac{\theta_c \pi}{180}\right) \sin\left(\frac{\phi_c \pi}{180}\right), \textbf{(1.9)}$$

The orientation tensor, in itself, is not very informative from a visual standpoint. Therefore, it is necessary to manipulate the orientation tensor in order to obtain a better understanding of the fiber orientation. The eigenvalues and eigenvectors of the orientation tensor must be calculated. The tensor's eigenvectors are three unit vectors that are perpendicular to one another. These vectors serve to rotate the coordinate axes to more closely reflect the orientation of the fibers. Once the eigenvectors have been calculated, the corresponding eigenvalue for each eigenvector tells how oriented the fibers are along that particular eigenvector. These eigenvalues and eigenvectors provide the best description of the carbon nanofiber orientation.

While it is important to know the general properties of a material that has been created, it would be even more advantageous if it were possible to predict those properties before the material is even processed. The ultimate goal of this project is to create a model that links the material's physical properties to the orientation of the carbon nanofibers. In turn, then, if it were possible to know the processing parameters that would yield a certain orientation tensor, the process could theoretically be tuned using the prediction model to create a material whose properties fit the needs of the manufacturer. The overall project described here could take many years to accomplish, therefore the time scale of this particular study is significantly smaller. This study mainly focuses on characterizing the relationship between nanofiber orientation and two main physical properties: tensile strength and electrical conductivity.

2) Literature Review

2.1) Nanofiber-Reinforced Polymer Materials

Much research has been conducted on nanofiber-reinforced polymer materials. Wang et al. also studied the polystyrene/carbon nanofiber system (1). They mainly addressed rheological properties of the material, showing that the material's viscoelastic moduli and melt viscosity tend to increase as the concentration of nanofibers in the material increases. This group also showed that the polystyrene and the carbon nanofibers have a negligible amount of interaction with one another. Finally, they were able to create a model that predicted several rheological properties as functions of variables like fiber length and mass concentration of carbon nanofibers.

Other groups have studied similar properties with systems other than polystyrene and carbon nanofibers. Du et al. studied a system of single-walled carbon nanotubes in poly(methyl methacrylate) (2). While their main focus was on rheology, they also looked at the electrical conductivity of the material. They found that the material had a percolation threshold of 0.39 wt% carbon nanotubes. This percolation threshold means that the material will experience no appreciable increase in electrical conductivity if the carbon nanotubes are present in less than 0.39 wt%. Electrical conductivity was found to increase monotonically with increasing concentration of nanotubes. Similarly, Hu et al. studied the electrical properties of multi-walled carbon nanotubes in poly(ethylene terephthalate) (3). They also found a relatively low percolation threshold for electrical conductivity, at approximately 0.9 wt% carbon fiber. However, Lozano et al. studied the electrical properties of vapor-grown carbon fibers in polypropylene, and obtained a percolation threshold for electrical conductivity at approximately 18 wt% carbon fiber

(4). This percolation threshold is significantly higher than that obtained by the previous two groups and could be due to the fact that different polymer materials and different types of carbon fiber were used in each study. Lozano's group also found that their material was highly suitable for electrostatic discharge applications.

Instead of looking at electrical conductivity, Shi et al. studied the rheological and mechanical properties of a poly(propylene fumarate)/single-walled carbon nanotube system (5). They tested only very small concentrations of nanotubes (<0.20%), and they found that the compressive and flexural strength encounter a maximum for nanotube concentrations of about 0.05 wt%. They also found that functionalizing the carbon nanotubes, i.e. subjecting the nanotubes to a reaction in order to add a new functional group, had no significant effect on the properties of the material.

2.2) Mechanical Properties

Like Shi et al., many other groups have studied the mechanical properties of nanofiber-reinforced polymer materials. Thostenson and Chou studied the tensile behavior of multi-walled carbon nanotubes in polystyrene (6). They used only one concentration of nanotubes (5 wt%) and a control material; however, they varied the alignment of the nanotubes in the polystyrene by using different dies when extruding the material. They found that the tensile modulus increased when nanotubes were added, and that the increase in tensile strength was greatly magnified when the nanotubes were highly aligned as opposed to randomly dispersed.

Some of the findings concerning the most favorable concentration of carbon fibers have been contradictory. Blond et al. used a system of multi-walled carbon nanotubes in poly(methyl methacrylate), and they found that mechanical properties tend

to decline if the concentration of nanotubes goes above 0.5 wt% (7). They postulated that this decrease in tensile strength was probably due to the nanotubes agglomerating in the material. However, Chen et al. found that, for a blend of multi-walled carbon nanotubes and poly(vinyl alcohol), the material showed the greatest tensile strength at a nanotube concentration of 9.1 wt% (8). They maintain that their dispersion of the nanotubes was made more effective by treating the nanotubes with strong acid before commencing the sonication process.

2.3) Electrical Properties

One of the major advantages of using carbon nanofibers in polymer composites is the upgrade in electrical conductivity. The amount of carbon nanofiber needed to provide a significant increase in electrical conductivity has been studied by Wu et al (9). This group found that the percolation threshold was about 2-3 vol% carbon nanotubes in unsaturated polyester resin, meaning that above this volume fraction the electrical conductivity increased appreciably. Sundaray et al., however, saw a nearly immediate increase (10). The conductivity of their material rose approximately ten orders of magnitude with less than 0.1 wt% of multi-walled carbon nanotubes added to a fiber of poly(methyl methacrylate). However, these multi-walled nanotubes were well-aligned in the direction of the fiber, which may explain the large rise in conductivity.

In a different type of experiment, Martin et al. explored the effects of current type (direct or alternating) on the orientation of multi-walled carbon nanotubes in an epoxy material (11). They found that applying an alternating current to this composite material resulted in a more uniform alignment of nanotubes than applying a direct current. Materials that were subjected to alternating current had higher electrical conductivities

than those subjected to direct current, suggesting that perhaps the increased alignment of the nanotubes correlated with the increase in conductivity. It was also found that the more current that was applied to the material, the higher the material's conductivity would be.

3) Experimental Procedures

3.1) Sample Preparation

Samples were made for testing using two different methods: compression molding and injection molding. The compression-molded samples were made with Fina brand polystyrene, produced by Atofina, and Pyrograf III carbon nanofibers, produced by Applied Sciences. The polystyrene had a density of 1,000 g/m^3, a weight average molecular weight of 200,000, and a polydispersity index of 2.4. The material for the samples was made in a DACA Instruments twin-screw microcompounder at 200°C with a screw rotation rate of 250 rpm. The material mixed in the microcompounder for four minutes. This melt blending method was used to produce material of 0, 2, 5, or 10 wt% carbon nanofibers. This material, which emerged from the microcompounder in the form of small pellets, was compression molded into various shapes. Some of the samples were discs, which were 25 mm in diameter and 0.5-1 mm thick. The other main type of sample was a rectangular rod, which is 52 mm long, 7 mm wide, and 1.55 mm thick. Both types of samples were made on a hot press at 200°C. The appropriate mold was filled with pellets and placed on the press for 15 minutes, allowing the pellets to melt. After 15 minutes, the pressure was quickly applied and released four times to release air bubbles in the mold. The pressure was reapplied and held for ten minutes, after which time the heat to the press was turned off. The sample temperature was allowed to fall below 100°C, the glass transition temperature. Once the samples had cooled, the pressure was released and the samples were removed from the mold. They were placed in a vacuum oven at 70°C for at least 24 hours to ensure that they did not absorb any moisture from the surrounding air.

The injection-molded samples were made using two different methods. The smaller samples were composed of the same pellets that were made in the microcompounder for compression molding. The pellets were injection molded into 25 mm diameter discs that were 0.5-1 mm thick. The equipment used was a micro-injection molder from DACA Instruments. The pellets were melted in the injection molder barrel at 200°C for 15 minutes. They were then injected into a mold, producing one sample for each injection. Pressure was maintained for several seconds after injection to prevent deformation of the sample.

The larger injection-molded samples were composed of Styron brand polystyrene, produced by Dow Chemical, and the same Pyrograf III carbon nanofibers used in the melt blending procedure. The density of the polystyrene is known to be 1,040 g/m^3; however, the weight average molecular weight and polydispersity index are both proprietary information that is not readily obtained. Before injection molding could take place, the polystyrene and carbon nanofibers had to be mixed together in a twin-screw extruder. The materials were fed to a Leistritz MIC 27 GL/40D twin-screw extruder. The barrel was held at 200°C, and the screws turned at a rate of 20 rpm. The material emerged from the extruder in three different strands, which were cooled in a water bath as they continued to flow. Once the strands reached the end of the water bath, they entered a chopper, where they were cut into small pellets. These pellets were used in the injection molding procedure, which utilized a Sumitomo C560 injection molder. The barrel temperature was set to 450°F (232°C), while the mold itself was held at a temperature of 132°F (56°C). Four different injection speeds were used: 0.75, 1.5, 2.25,

and 3 in/s. After injection, the samples were cooled for 60 s before being removed from the mold.

3.2) Tensile Strength Testing

Tensile strength testing was performed on an Instron microtester. The sample bars, which were made with the Sumitomo C560 injection molder using the procedure described above, were 7 in long and followed the ASTM standard for shape. The samples were stretched at a rate of 0.2 in/s using a 50 kN load cell. The test used was the ASTM D638 standard test. The sample bar was placed inside the clamps, and an extensiometer was attached to the sample to transmit tensile data to the computer. The sample was then stretched until it fractured, after which the sample was removed and the clamps were returned to their original position for the next test.

3.3) Electrical Resistivity Testing

Electrical resistivity testing was conducted using a Keithley 8009 resistivity measurement device. Two basic types of tests were used. For smaller samples that did not cover the entire surface of the electrode, a Teflon mask was placed around the sample. This mask, which was made of a very resistive material, covered the rest of the electrode. The samples that required this mask were the compression-molded samples and the smaller injection-molded samples. The test itself consisted of eleven 15-second segments. For each segment, a potential difference of 500 V was applied across the electrodes. At the end of each segment, the direction of the potential difference was switched. For the first three segments, no measurements were taken by the computer. For the next three segments, measurements were taken but discarded by the computer.

Finally, for the last five segments, data were collected and saved. The sample's resistivity was determined to be the average of these five data points.

For the larger injection-molded samples, which had a diameter of 5.4 cm, no mask was required because the samples covered the entire electrode. However, the above test was found to be ineffective, as the data it yielded were erratic and sometimes made no physical sense (e.g. negative electrical resistivities). Therefore, a second test was used. This test, as dictated by an ASTM standard, consisted simply of applying a 500 V potential difference for 60 seconds. At the end of the test, the current flowing through the sample was measured, and the current was converted into a resistivity by using the following equation:

$$\rho = \frac{A \cdot V}{I \cdot t}, \textbf{ (3.3.1)}$$

where ρ is the volume resistivity (in Ω-cm), A is the area of the electrode (22.9 cm^2), V is the applied voltage (500 V), I is the current (in A) through the sample after 60 seconds, and t is the sample thickness (0.31 cm).

3.4) Sample Deformations

To test the effects of deformation on carbon nanofiber orientation, samples were made to undergo two different types of deformation. The first type of deformation was to subject a compression-molded disc-shaped sample to rotational shearing. This shearing was performed on an ARES Rheometer from TA Instruments. The rheometer used a parallel plate geometry, and the plates were 25 mm in diameter. The temperature was set to 200°C, and the plates were allowed to heat for 10 minutes. Then the sample was loaded onto the plates and allowed to heat for 15 minutes. The shearing was then performed at various shear rates: 0.1, 1, and 10 s^{-1}. The samples were sheared to a total

strain of 40, meaning that the tests lasted for 400, 40, and 4 seconds, respectively. At present, all necessary samples have been sheared; however, no TEM images of these samples have yet been taken.

The second type of deformation used compression-molded rod-shaped samples. The rods were subjected to extensional flows using an RME Rheometer from Rheometrics Scientific. The samples were allowed to melt at 170°C for 15 minutes, after which they were stretched to a total strain of 0.5, 1, or 2. The extensional rate was 0.1 s^{-1}, so the tests lasted for 5, 10, or 20 seconds, respectively. Once these samples were sheared, a small section of each sample was prepared for TEM imaging.

3.5) Transmission Electron Microscopy

Several samples underwent transmission electron microscopy (TEM) in order to better understand the orientation of the carbon nanofibers in the material. Samples were cut in a microtome using a diamond knife. The thickness of the slices was 200 nm, and the cut was made at an angle of 20° from the original direction of material flow. The TEM images were taken by a Tecnai G2 Spirit apparatus, which operated at 120 kV. Some images were also taken after the sample was tilted approximately 40° from the horizontal. Analysis of the images was performed in AutoCAD using a program written by Jianhua Xu.

4) Results and Discussion

4.1) Tensile Strength of Injection-Molded Samples

For the tensile strength experiments, the two main variables that were studied were injection speed and composition. Several trials were done at each set of conditions, and the average modulus value for each injection speed and composition was determined. Figure 4.1.1 below shows how the modulus varies with injection speed and composition.

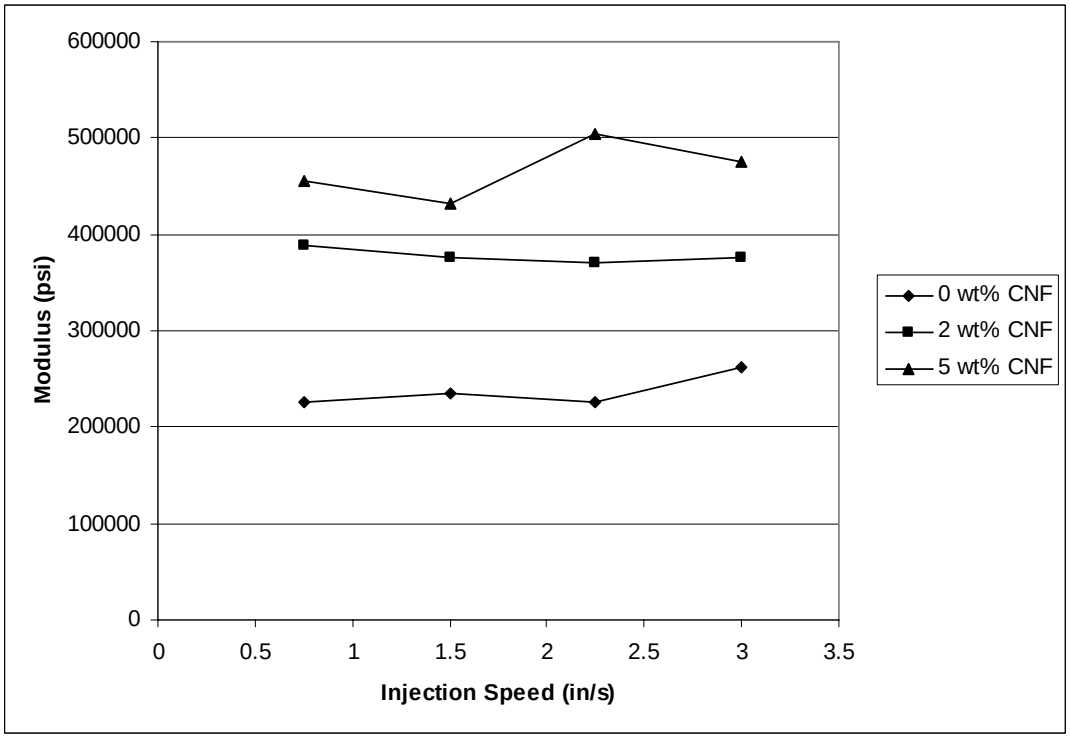

Figure 4.1.1: Tensile Modulus for Injection-Molded Samples

By examining Figure 4.1.1, it is easily observed that modulus tends to increase as more carbon nanofibers are added to the material. However, no correlation between modulus and injection speed can be readily determined. In fact, analysis of variance shows that composition has a highly significant effect on modulus, whereas it is highly improbable from the experimental data that injection speed has a significant effect.

The same tests that were used to acquire the tensile modulus data also recorded tensile strength data for each sample. The results of the tensile strength test are summarized in Figure 4.1.2 below.

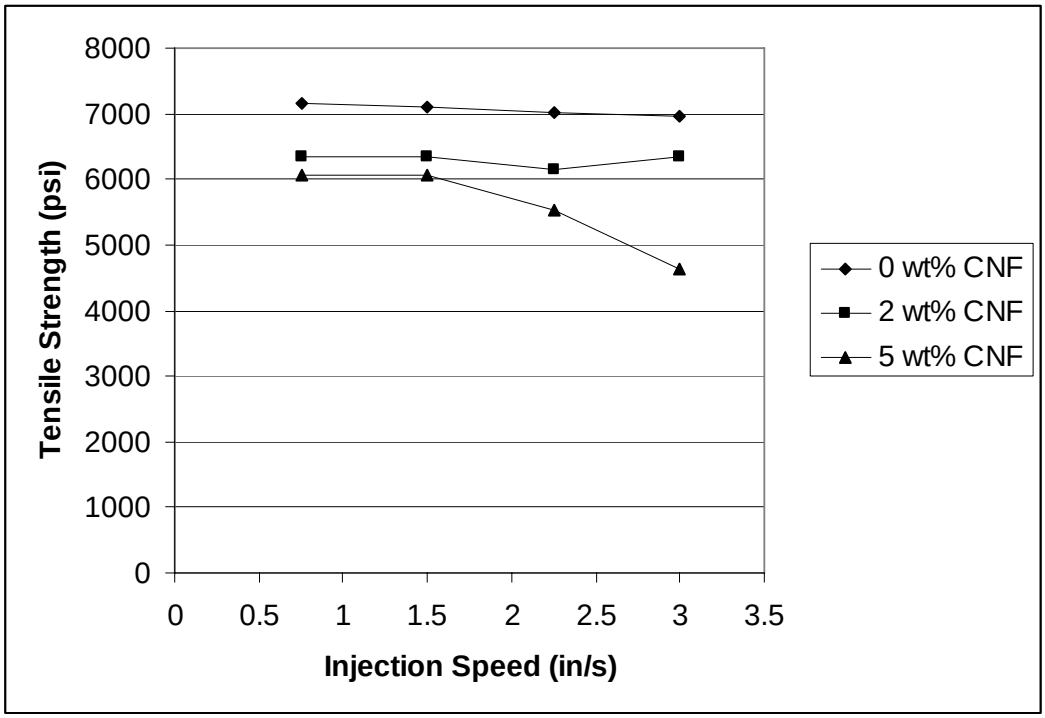

Figure 4.1.2: Tensile Strength for Injection-Molded Samples

In this experiment, the opposite trend from the tensile modulus experiment is observed: as more carbon nanofibers are added, the tensile strength decreases significantly. Additionally, in this experiment, composition is not the only significant variable that affects the tensile strength. Analysis of variance shows that composition, injection speed, and the interaction between composition and injection speed all have a significant effect on the tensile strength of a sample.

4.2) Electrical Resistivity

In order to study the effects of fiber orientation on electrical properties, the electrical resistivities of both compression-molded and injection-molded samples were

tested. Without being able to see the actual fiber orientations, it can be theorized that the compression-molded samples have fibers that are mostly randomly aligned, while the injection-molded samples tend to show more radial alignment of the fibers. The first set of resistivity measurements included samples with either 0 wt% carbon nanofibers or 2 wt% nanofibers. The results of this test are summarized in Figure 4.2.1 below.

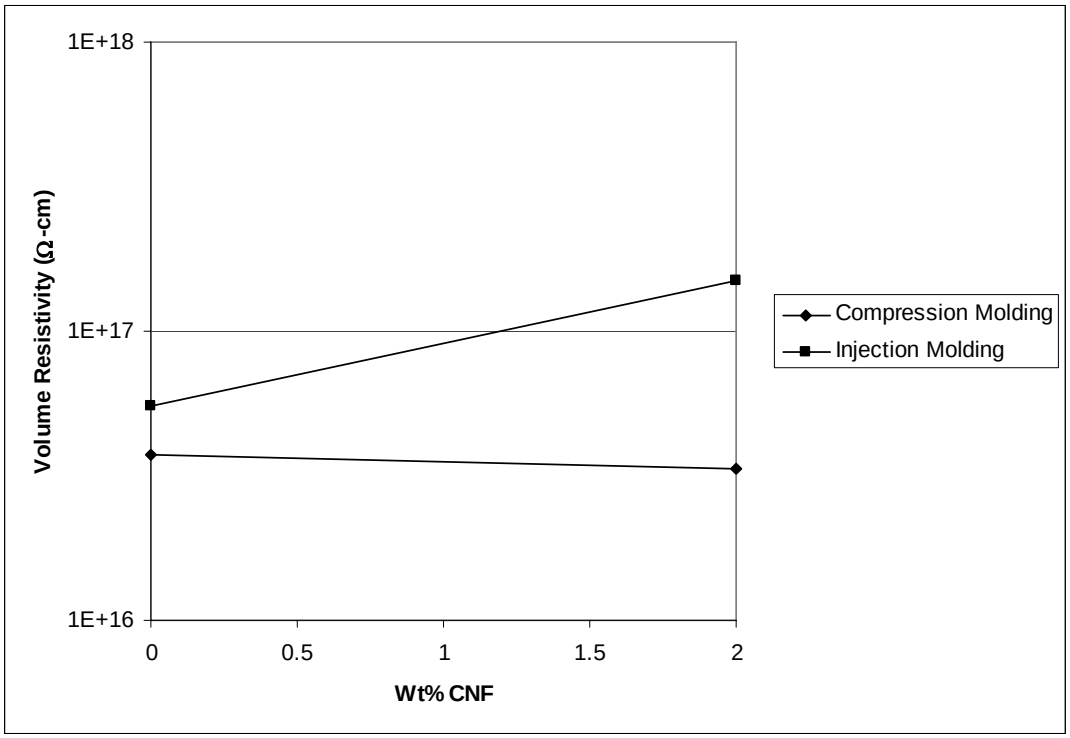

Figure 4.2.1: Volume Resistivity of Compression Molding vs. Injection Molding, 0-2 wt% CNF

By looking at Figure 4.2.1, the logical conclusion would be that the type of molding process significantly affects the resistivity of a sample, while the composition does not have a significant effect. Analysis of variance for this experiment would appear to confirm this conclusion. However, the conclusion changes if a wider range of compositions is used. Figure 4.2.2 summarizes the results of a similar experiment, in which the composition ranges from 0 wt% carbon nanofibers to 10 wt% nanofibers.

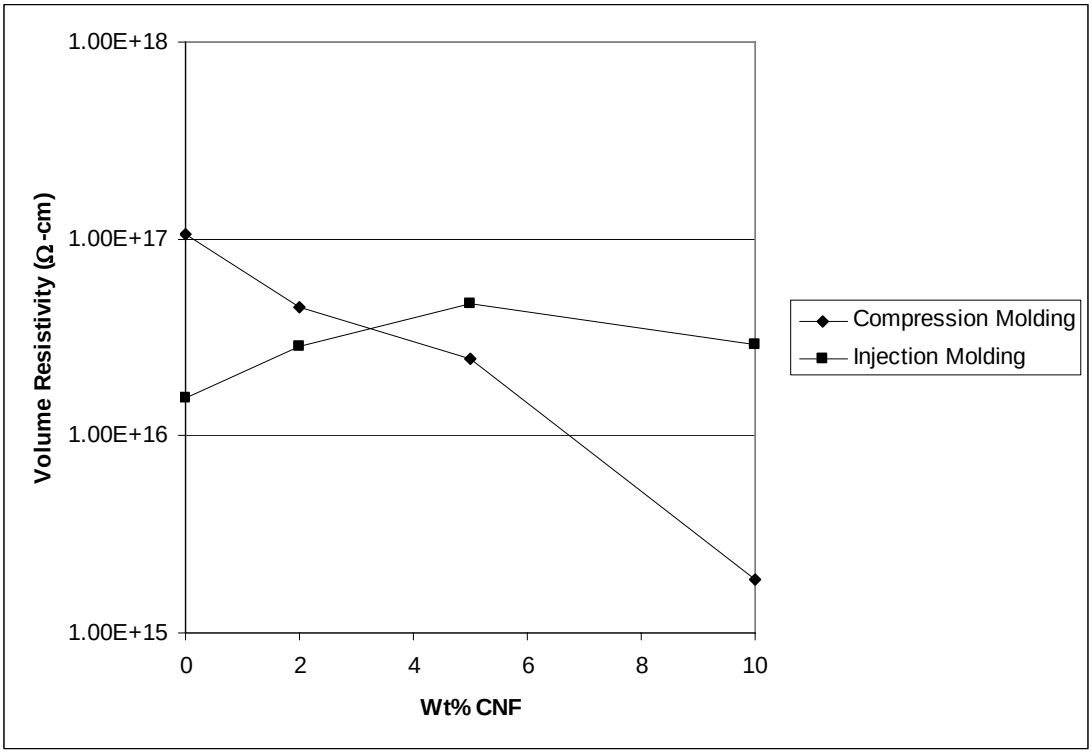

Figure 4.2.2: Volume Resistivity of Compression Molding vs. Injection Molding, 0-10 wt% CNF

The analysis of variance for the experiment summarized in Figure 4.2.2 leads to different conclusions than those from the previous experiment. Now it is observed that the composition of the material does have a significant effect on electrical resistivity, and the processing method itself is not a significant effect. However, the interaction between processing method and composition does have a significant effect on resistivity.

In a different experiment, the goal was to determine if changing the speed of injection has any effect on electrical resistivity. To accomplish this purpose, four different injection speeds were studied: 0.75, 1.5, 2.25, and 3 in/s. Each of these speeds included samples composed of either 0, 2, or 5 wt% carbon nanofibers. Two samples at each combination of composition and injection speed were tested, yielding 24 data points in all. The results of this test are shown in Figure 4.2.3.

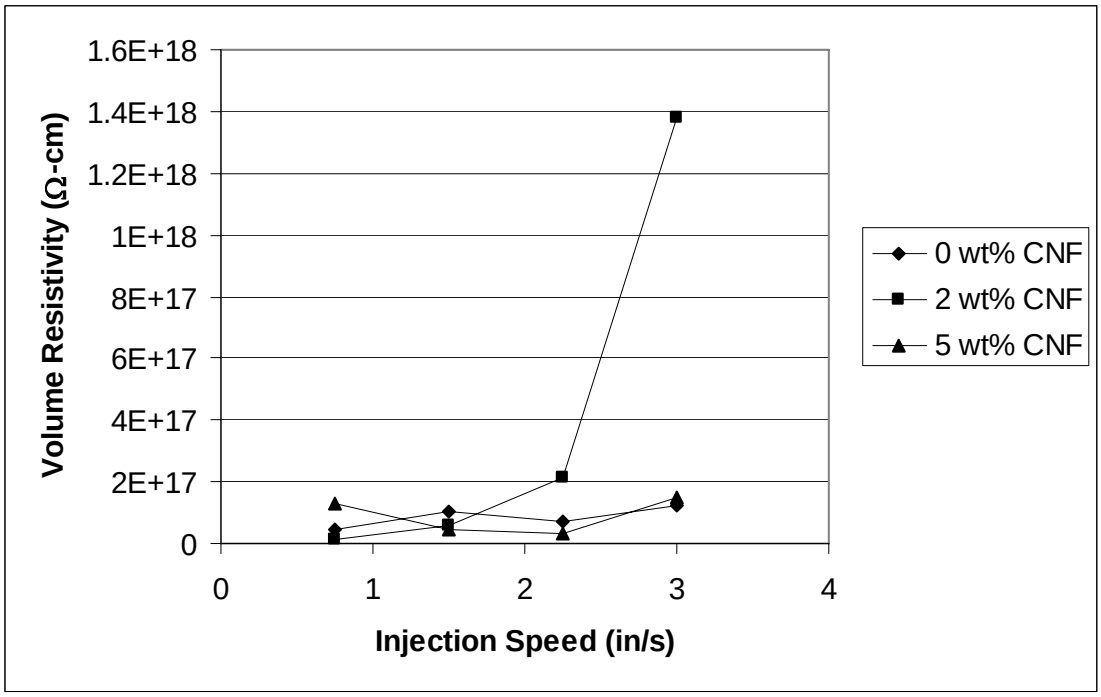

Figure 4.2.3: Volume Resistivities of Injection-Molded Samples with Different Injection Speeds

Analysis of variance for this experiment suggests that neither composition nor injection speed significantly affect the volume resistivity of a sample. This finding could lead to at least two different conclusions. Either the injection speed does not significantly affect the orientation of the carbon nanofibers, or the range of injection speeds was so small that no significant difference could be detected. It is also possible that not enough samples were tested to give a clear idea of the effects of processing variables on resistivity, though the maximum number of tests was performed, given the number of available samples.

4.3) Orientation Tensor Calculations

As described in Section 3.4, four samples were subjected to shear in an extensional rheometer. Each sample underwent a different amount of total strain, and the orientation tensors for each sample were calculated. The first sample was subjected to no strain, and it can be seen in Figure 4.3.1.

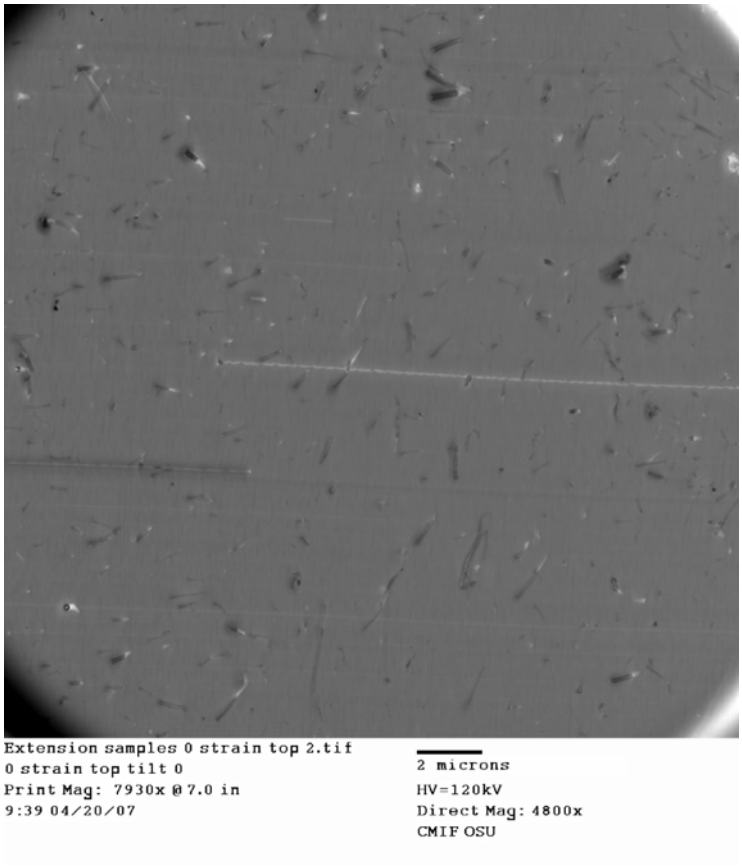

Figure 4.3.1: TEM Image of Sample with Total Strain = 0

In each image, the flow direction is perpendicular to the white line across the sample and is rotated 70° out of the plane. In Figure 4.3.1, there actually is no flow direction since this sample was not subjected to extensional shear, but the same standard is used to keep the data analysis consistent with the other samples. Each dark gray or black line is a carbon nanofiber. These fibers were marked in AutoCAD, and analysis of these fibers yielded the following orientation tensor:

$$a = \begin{bmatrix} 0.33 & -0.31 & 0.11 \\ -0.31 & 0.30 & -0.05 \\ 0.11 & -0.05 & 0.36 \end{bmatrix}$$

The diagonal entries of the orientation tensor provide some insight into the fiber orientation. If the fibers are completely randomly oriented, it would be expected that the

three diagonal entries would all be equal to 1/3. In this case, the diagonal entries signify that the fibers are very close to random orientation. However, as has been previously stated, the orientation tensor itself is not the final step in the orientation calculation. Now the eigenvalues and eigenvectors must be calculated. They are as follows:

$$v_1 = \begin{bmatrix} .7003 \\ .7043 \\ -.1162 \end{bmatrix}, \lambda_1 = 0$$

$$v_2 = \begin{bmatrix} -.1731 \\ .3254 \\ .9296 \end{bmatrix}, \lambda_2 = 0.332$$

$$v_3 = \begin{bmatrix} .6925 \\ -.6309 \\ .3498 \end{bmatrix}, \lambda_3 = 0.668$$

The eigenvectors give the directional axes for the fiber orientation, and each eigenvalue gives the magnitude of the orientation in the direction of its corresponding eigenvector.

The next sample to be analyzed was subjected to a total strain of 0.5; that is, after the sample was extended, its new length was 1.5 times its original length. The TEM image of this sample is shown in Figure 4.3.2.

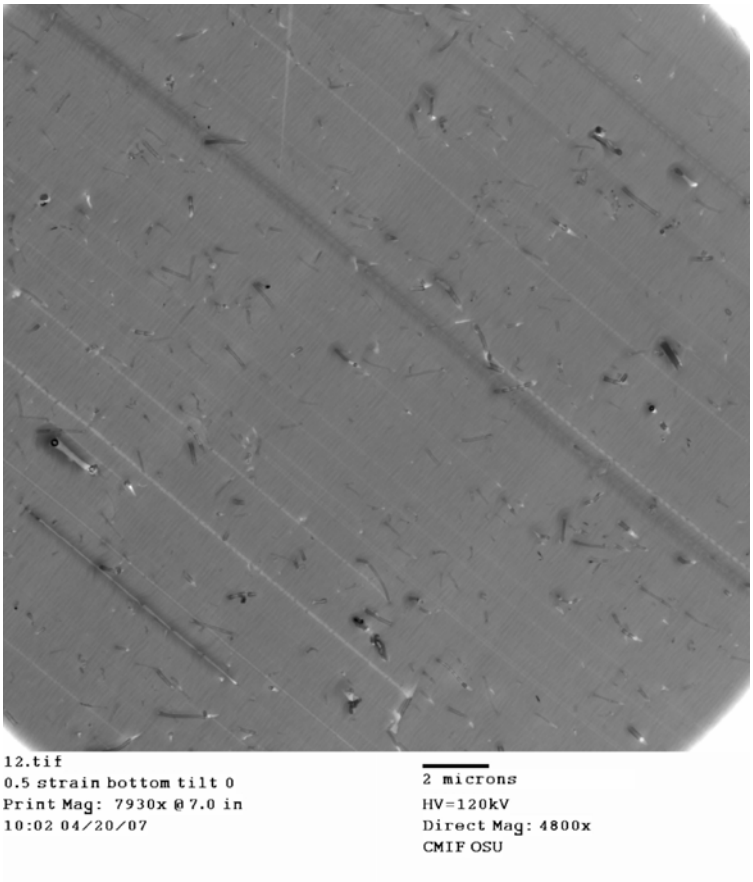

Figure 4.3.2: TEM Image of Sample with Total Strain = 0.5

Visual inspection of Figure 4.3.2 shows that the carbon nanofibers are starting to be more aligned in the flow direction. The calculated orientation tensor provides further evidence for this phenomenon:

$$a = \begin{bmatrix} 0.36 & -0.36 & 0.06 \\ -0.36 & 0.36 & -0.02 \\ 0.06 & -0.02 & 0.27 \end{bmatrix}$$

This tensor gives the following eigenvectors and eigenvalues:

$$v_1 = \begin{bmatrix} .7090 \\ .6974 \\ -.1047 \end{bmatrix}, \lambda_1 = -.003$$

$$v_2 = \begin{bmatrix} -.0127 \\ .1611 \\ .9868 \end{bmatrix}, \lambda_2 = 0.266$$

$$v_3 = \begin{bmatrix} .7051 \\ -.6983 \\ .1231 \end{bmatrix}, \lambda_3 = 0.727$$

The third sample had a total strain of 1, so its final length was twice its original length. The TEM image of this sample is presented in Figure 4.3.3.

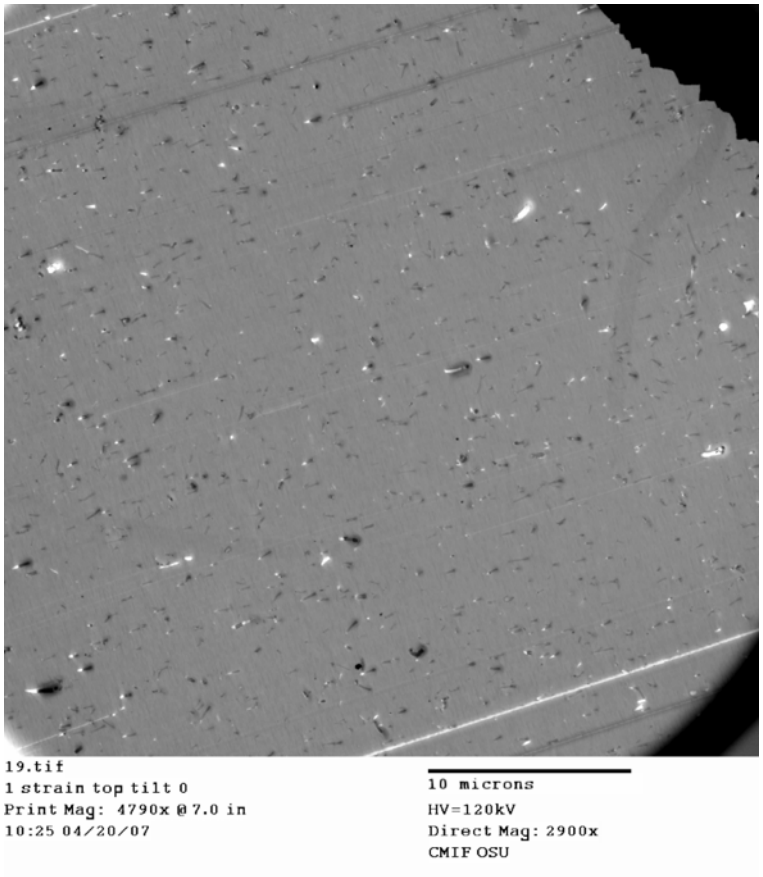

Figure 4.3.3: TEM Image of Sample with Total Strain = 1

The carbon nanofibers continued to become more aligned in both the 1-direction and the 2-direction, as confirmed by the following orientation tensor:

$$a = \begin{bmatrix} 0.41 & -0.41 & 0.08 \\ -0.41 & 0.42 & -0.05 \\ 0.08 & -0.05 & 0.18 \end{bmatrix}$$

Once again, the eigenvalues and eigenvectors for this orientation tensor were calculated.

$$v_1 = \begin{bmatrix} .7155 \\ .6866 \\ -.1288 \end{bmatrix}, \lambda_1 = .0021$$

$$v_2 = \begin{bmatrix} -.0045 \\ .1889 \\ .9820 \end{bmatrix}, \lambda_2 = 0.1700$$

$$v_3 = \begin{bmatrix} .6986 \\ -.7020 \\ .1383 \end{bmatrix}, \lambda_3 = 0.8378$$

The final sample underwent a total strain of 2, so the final length was three times the original length. The TEM image of this sample can be found in Figure 4.3.4.

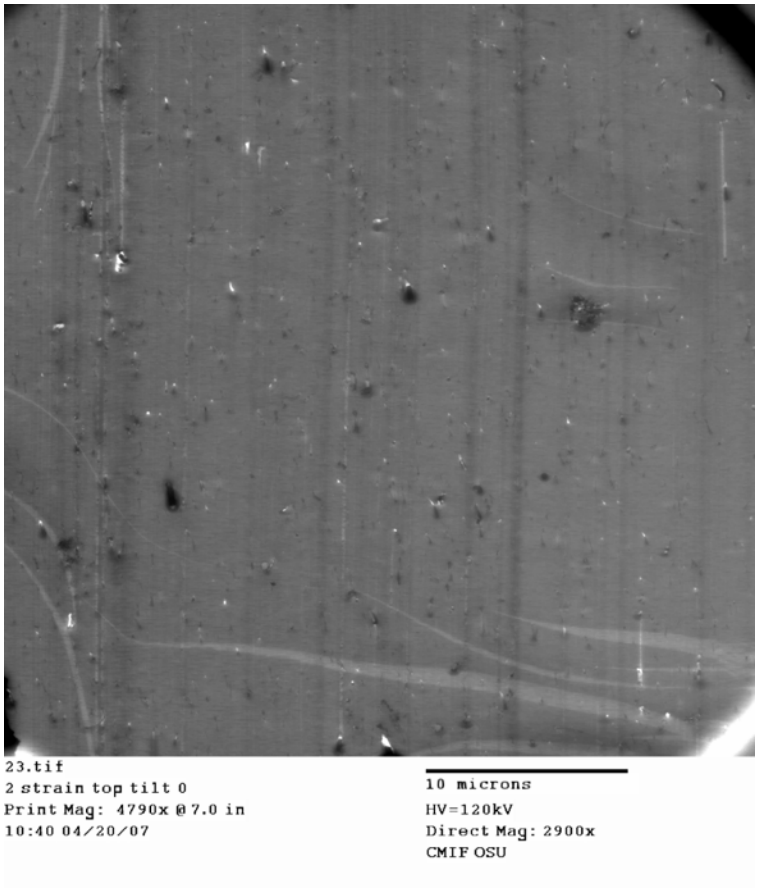

Figure 4.3.4: TEM Image of Sample with Total Strain = 2

A problem that was encountered with this sample was the fact that the material was becoming very stretched out at a total strain of 2, and so the surface was becoming less uniform than the previous samples. Therefore, it was more difficult in this sample to locate nanofibers and tell which direction they were pointing. Nonetheless, enough fibers could be discerned to calculate an orientation tensor, and subsequently the eigenvalues and eigenvectors:

$$a = \begin{bmatrix} 0.42 & -0.41 & 0.11 \\ -0.41 & 0.40 & -0.09 \\ 0.11 & -0.09 & 0.17 \end{bmatrix}$$

$$v_1 = \begin{bmatrix} .7063 \\ .7029 \\ -.0843 \end{bmatrix}, \lambda_1 = -.0012$$

$$v_2 = \begin{bmatrix} -.0859 \\ .2033 \\ .9753 \end{bmatrix}, \lambda_2 = 0.1415$$

$$v_3 = \begin{bmatrix} .7027 \\ -.6816 \\ .2040 \end{bmatrix}, \lambda_3 = 0.8496$$

When this orientation tensor is compared to the one for the sample with a total strain of 1, a new trend emerges. Now the alignment of fibers has increased only in the 1-direction, with the alignment in the 2-direction decreasing for the first time. While this result is closer to what might be expected, it is important not to draw too many conclusions based on it. Not only are the increase in a_{11} and the decrease in a_{22} both very small, but the surface of this sample was also not as clear as the other samples. A more likely explanation of this orientation tensor would be that, after the total strain reaches a certain value, the elongation of the sample ceases to have a significant effect on the fiber orientation. The small difference between this orientation tensor and that for the sample with a total strain of 1 would seem to substantiate that explanation.

One problem that must be overcome when analyzing the orientation of carbon nanofibers is a certain level of ambiguity that emerges when θ is calculated. Examine the circled fiber in Figure 4.3.5 below.

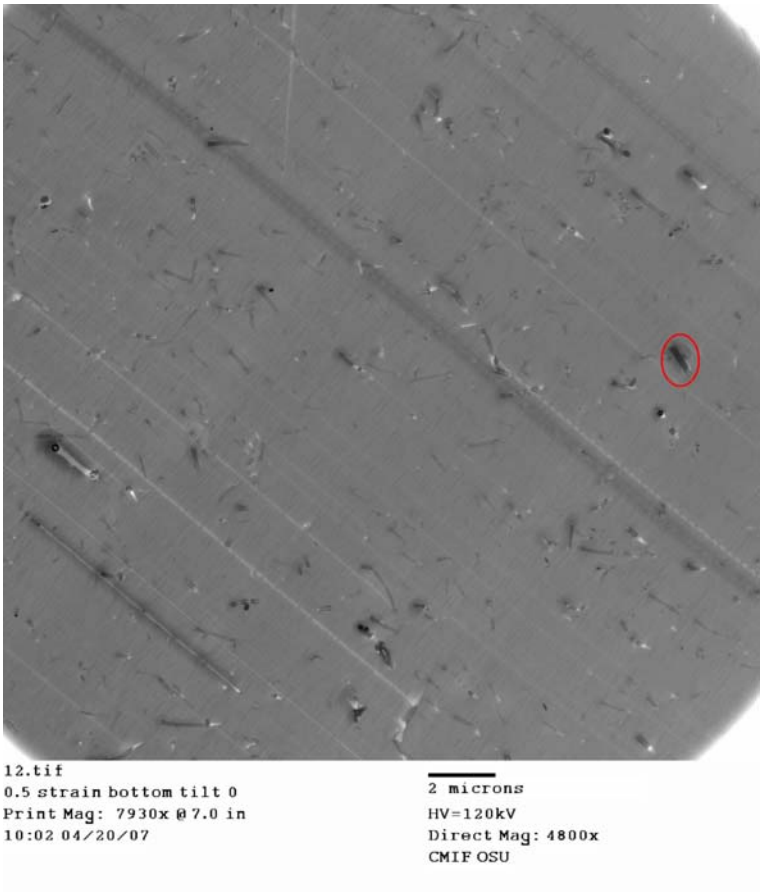

Figure 4.3.5: Fiber in Normal Sample

This fiber has a projected length of 0.96 μm, and when Equation 1.1 is applied, it is calculated that θ=78.2°. However, it is not known which end of the fiber is pointing up out of the picture, so the angle is really ±78.2°. In general, this ambiguity can be solved by tilting the sample and taking another image. Figure 4.3.6 shows this same sample tilted at an angle of 39° from the horizontal.

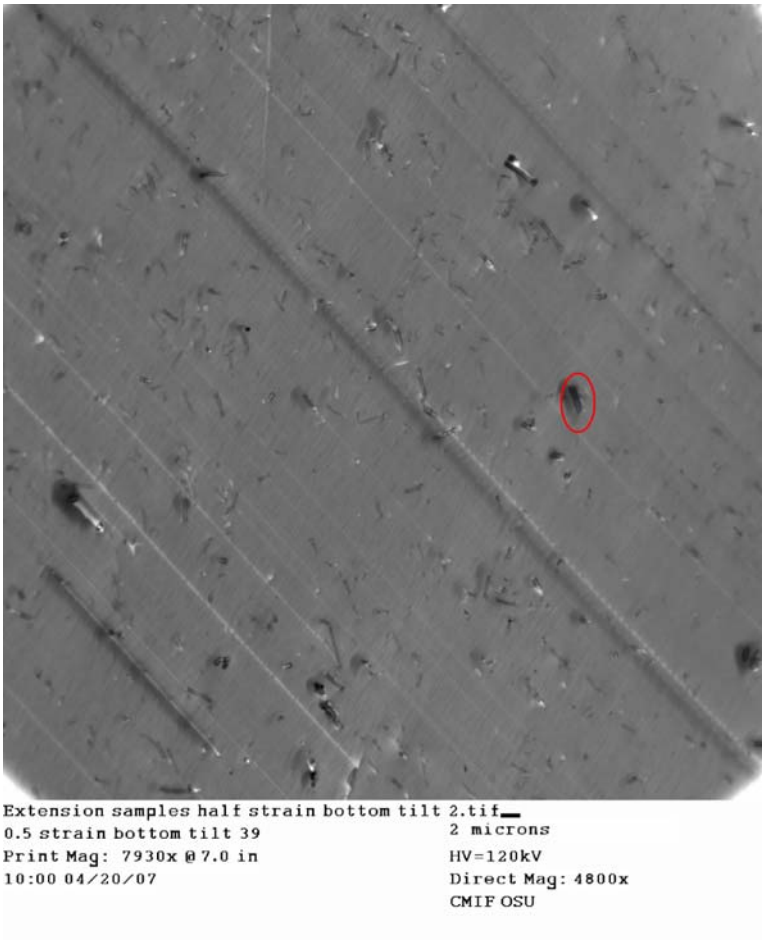

Figure 4.3.6: Fiber in Tilted Sample

The sample was tilted 39°, with the right side of the image having been rotated out of the page. The fiber appears to have rotated clockwise within the plane as the image was tilted, suggesting that the bottom end of the fiber is the end pointing out of the page. As long as a uniform standard is maintained, positive and negative out-of-plane angles can be calculated.

Two problems exist with the above method. The first difficulty, from a purely computational standpoint, is that this process would be difficult to automate. An AutoCAD code can be used to calculate lengths and in-plane angles for each fiber. However, using AutoCAD to compare corresponding fibers in two different images could

prove to be extremely difficult. Second, the above method for determining whether θ is positive or negative must be altered for certain fibers. Observe the circled fiber in Figure 4.3.7 below.

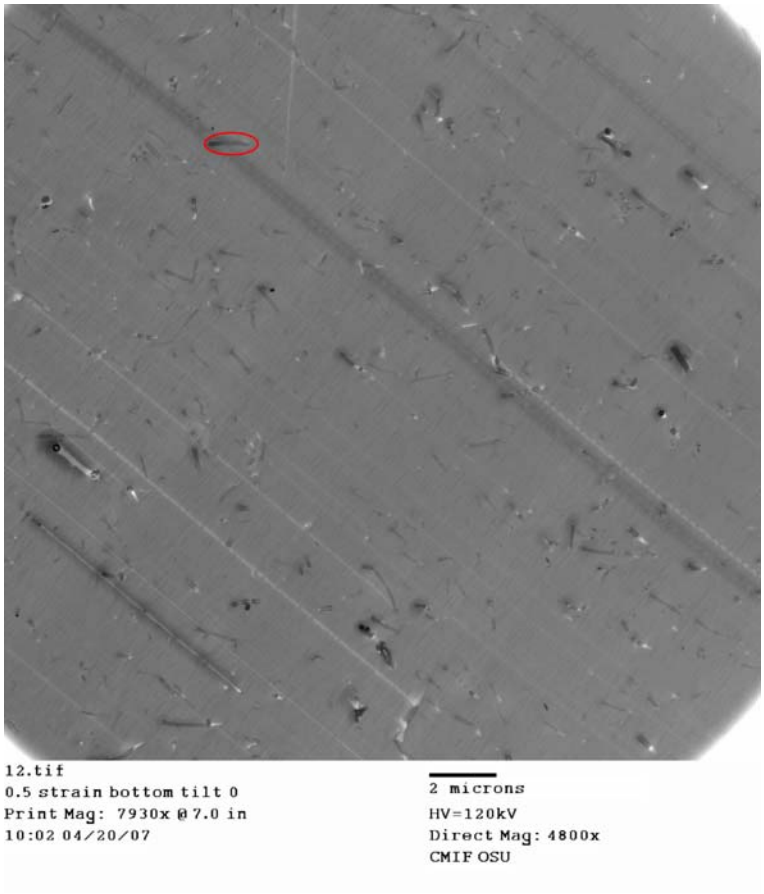

Figure 4.3.7: Horizontal Fiber in Normal Sample

The circled fiber has a projected length of 1.28 μm, and when Equation 1.1 is applied, it is determined that θ=81.1°. Now observe what happens when the sample is tilted in Figure 4.3.8.

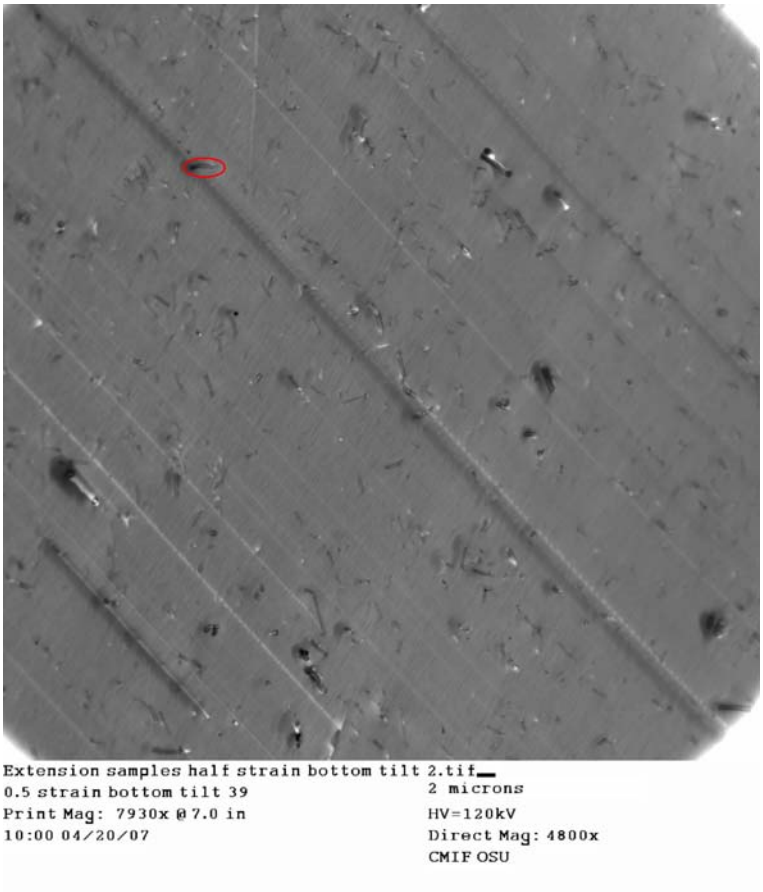

Figure 4.3.8: Horizontal Fiber in Tilted Sample

Since the fiber began at an in-plane angle very close to horizontal, the in-plane angle did not change appreciably (or at all) when the sample was tilted. Now a different method must be used to determine which end of the fiber points out of the page. It can be observed that the fiber's projected length became shorter when the sample was tilted. From this information, it can be deduced that the right side of the fiber is pointing out of the page. If this calculation process is eventually automated, the code should use some combination of in-plane angle changes and projected length changes to determine whether the out-of-plane angle is positive or negative; however, it must also be ensured that AutoCAD (or whichever program is being used) can compare corresponding fibers in the two images perfectly, or this approach cannot be automated.

5) Summary and Conclusions

A system of polystyrene and carbon nanofibers was studied to explore the effect of nanofiber orientation on the physical properties of the material. Orientation was varied by using several different processing methods, including compression molding and two different injection molding methods. The physical properties that were tested were tensile strength, tensile modulus, and electrical resistivity. It was found that the tensile strength of the material tended to decrease as the injection speed or the mass fraction of carbon nanofibers increased. The tensile modulus, on the other hand, was found to increase as more carbon nanofibers were added to the material, and no correlation between tensile modulus and injection speed could be determined. The electrical resistivity tests revealed that resistivity depends on the composition of the material and the processing method, although no trend relating resistivity to injection speed was discerned.

Several samples of 2 wt% carbon nanofibers were subjected to extensional strain to study the effects of shear stress on the orientation tensor. It was found that both a_{11} and a_{22} tended to increase as the total strain increased, and a_{33} tended to decrease. At a certain level of strain, the effects of the shear stress ceased to significantly affect the orientation of the fibers. It was also determined that the ambiguity in the out-of-plane angle θ could be eliminated by tilting the sample, taking a second image, and comparing the two images.

Future work should include, most importantly, finding a method to automate the process of comparing two TEM images to determine the definitive orientation tensor. Other areas of continued study would include exploring different fiber orientations and

material processing methods, as well as possibly altering the chemical composition of the carbon nanofibers to see if adding different functional groups changes how the nanofibers affect the properties of the material.

6) References

1) Wang, Y.; Xu, J.; Bechtel, S.; Koelling, K. *Rheologica Acta* **2006**, 45, 919-941.
2) Du, F.; Scogna, R. C.; Zhou, W.; Brand, S.; Fischer, J. E.; Winey, K. I. *Macromolecules* **2004**, 37, 9048-9055.
3) Hu, G.; Zhao, C.; Zhang, S.; Yang, M.; Wang, Z. *Polymer* **2006**, 47, 480-488.
4) Lozano, K.; Bonilla-Rios, J.; Barrera, E. V. *Applied Polymer Science* **2001**, 80, 1162-1172.
5) Shi, X.; Hudson, J. L.; Spicer, P. P.; Tour, J. M.; Krishnamoorti, R.; Mikos, A. G. *Nanotechnology* **2005**, 16, S531-S538.
6) Thostenson, E. T.; Chou, T.-W. *Physics D: Applied Physics* **2002**, 35, L77-L80.
7) Blond, D.; Barron, V.; Ruether, M.; Ryan, K. P.; Nicolosi, V.; Blau, W. J.; Coleman, J. N. *Advanced Functional Materials* **2006**, 16, 1608-1614.
8) Chen, W.; Tao, X.; Xue, P.; Cheng, X. *Applied Surface Science* **2005**, 252, 1404-1409.
9) Wu, S.-H.; Masaharu, I.; Natsuki, T.; Ni, Q.-Q. *Reinforced Plastics and Composites* **2006**, 25, 1957-1966.
10) Sundaray, B.; Subramanian, V.; Natarajan, T. S.; Krishnamurthy, K. *Applied Physics Letters* **2006**, 88, 143114.
11) Martin, C. A.; Sandler, J. K. W.; Windle, A. H.; Schwarz, M.-K.; Bauhofer, W.; Schulte, K.; Shaffer, M. S. P. *Polymer* **2005**, 46, 877-886.